Inorg. Chem. **2007**, *46*, 6891–6901

Syntheses of Homochiral Multinuclear Ru Complexes Based on Oligomeric Bibenzimidazoles

Jun Yin and Ronald L. Elsenbaumer*

Department of Chemistry and Biochemistry, The University of Texas at Arlington, Arlington, Texas 76019

Received November 12, 2006

The homochiral multinuclear Ru complexes of the oligomeric bibenzimidazoles were synthesized using Λ-[Ru(bpy)$_2$(py)$_2$][(–)-*O*,*O*′-dibenzoyl-L-tartrate]·12H$_2$O as an enantiomerically pure building block. The complexations proceed with the retention of configuration to provide well-defined mononuclear, dinuclear, tetranuclear, and octanuclear Ru complexes successfully. The optical purity and the absolute configurations of the complexes were determined by NMR and circular dichroism spectrometry. The rare X-ray structure of a tetranuclear complex Λ$_4$-[(Ru(bpy)$_2$)$_4$(bis(BiBzIm))](PF$_6$)$_4$ was resolved. The crystallographic analysis reveals that all the four Ru centers have Λ octahedral configurations, with a Ru–Ru separation of 5.509 Å across the bridging bibenzimidazole ligand, which maintains near coplanarity. The UV–vis spectroscopic and electrochemical properties of the homochiral multinuclear assemblies were studied, indicating weak electronic communications between the metal centers.

Introduction

Metal-complexed conjugated polymers have attracted significant attention in recent years.[1−5] The incorporation of transition metals has the potential to greatly expand the function and ultimate applications of conducting polymer systems. More specifically, there is a steady and growing effort to incorporate redox-active metal centers into conducting polymer structures to create highly efficient redox-modulated conductivity for sensory, catalytic, photochemical, and photoelectronic applications.[6−8]

Polymetallic assemblies which contains d^6 transition metal centers (e.g., Ru^{II}, Os^{II}), particularly coordinated to polypyridyl ligands, have been of great interest because of their favorable photophysical and redox characteristics.[9−12] However, an understanding of the interactive roles that the metal centers and the organic polymer backbone play is still in its early stages.[1,2] It has been demonstrated by Pickup and coworkers that the existence of superexchange interactions between metal centers coordinated to conjugated polymer backbones enhanced the rate of electron transport through the polymer in a series of Ru- and Os-complexed polybenzimidazoles with benzimidazole-pyridine or benzimidazole-pyrazine as the repeat units.[6] It was predicted that higher rates of electron transport could be achieved by better matching of orbital energies between the metal-based dπ orbitals and the polymer π or π* orbitals.

In order to probe the orbital interactions between metals and conjugated polymers, we have designed and successfully synthesized a series of novel oligomeric bibenzimidazoles

* To whom correspondence should be addressed. Tel: 1-817-272-1021. Fax: 1-817-272-2625. E-mail: elsenbaumer@uta.edu.

(1) Holliday, B. J.; Swager, T. M. *Chem. Commun.* **2005**, *1*, 23−36.
(2) Kingsborough, R. P.; Swager, T. M. *Prog. Inorg. Chem.* **1999**, *48*, 123−231.
(3) Liu, Y.; De Nicola, A.; Reiff, O.; Ziessel, R.; Schanze, K. S. *J. Phys. Chem. A* **2003**, *107*, 3476−3485.
(4) Liu, Y.; Li, Y.; Schanze, K. S. *J. Photochem. Photobiol. C: Photochem. Rev.* **2002**, *3*, 1−23.
(5) Pickup, P. G. *J. Mater. Chem.* **1999**, *9*, 1641−1653.
(6) (a) Cameron, C. G.; MacLean, B. J.; Pickup, P. G. *Macromol. Symp.* **2003**, *196*, 165−171. (b) Cameron, C. G.; Pickup, P. G. *Chem. Commun.* **1997**, 303−304. (c) Cameron, C. G.; Pickup, P. G. *J. Am. Chem. Soc.* **1999**, *121*, 11773−11779. (d) Cameron, C. G.; Pickup, P. G. *J. Am. Chem. Soc.* **1999**, *121*, 7710−7711. (e) Cameron, C. G.; Pittman, T. J.; Pickup, P. G. *J. Phys. Chem. B* **2001**, *105*, 8838−8844. (f) MacLean, B. J.; Pickup, P. G. *J. Mater. Chem.* **2001**, *11*, 1357−1363. (g) MacLean, B. J.; Pickup, P. G. *J. Phys. Chem. B* **2002**, *106*, 4658−4662.
(7) (a) Hayashida, N.; Yamamoto, T. *Bull. Chem. Soc. Jpn.* **1999**, *72*, 1153−1162. (b) Yamamoto, T.; Maruyama, T.; Zhou, Z.-H.; Ito, T.; Fukuda, T.; Yoneda, Y.; Begum, F.; Ikeda, T.; Sasaki, S.; et al. *J. Am. Chem. Soc.* **1994**, *116*, 4832−4845.
(8) Zhu, S. S.; Swager, T. M. *J. Am. Chem. Soc.* **1997**, *119*, 12568−12577.
(9) Balzani, V.; Juris, A.; Venturi, M.; Campagna, S.; Serroni, S. *Chem. Rev.* **1996**, *96*, 759−834.
(10) Juris, A.; Balzani, V.; Barigelletti, F.; Campagna, S.; Belser, P.; von Zelewsky, A. *Coord. Chem. Rev.* **1988**, *84*, 85−277.
(11) Kalyanasundaram, K. *Coord. Chem. Rev.* **1982**, *46*, 159−244.
(12) Kalyanasundaram, K. *Photochemistry of Polypyridine and Porphyrin Complexes*; Academic Press: London, 1992.

10.1021/ic062148a CCC: $37.00
Published on Web 07/21/2007

with 2,2′-bibenzimidazole as the repeat unit.[13] Our continuing effort on this project involves design and syntheses of well-defined polynuclear ruthenium complexes using these oligomeric bibenzimidazoles as the conjugated backbones.

There are several reasons for the choice of the polybibenzimidazoles as π-conjugated backbones:[5] They tend to be very robust and remain stable under considerable thermal and chemical stress;[14] The studies of binuclear benzimidazole complexes have shown that they possess significant electronic coupling between two metals.[15−17] In addition, removal of the imidazole NH protons would allow pH control of the electron density on the conjugated ligands and the corresponding metal complexes.[18−21]

Our initial attempts for the synthesis of the corresponding multinuclear Ru complexes using racemic $Ru(bpy)_2Cl_2$ as the building block met with limited success[22] because the polynuclear Ru complexes without the stereocontrol of each octahedral center have generally been isomeric mixtures. Thus, the isolation and characterization of these mixtures have been extremely difficult and complicated. This is particularly true when bidentate ligands are involved. In addition, X-ray crystal structures of multinuclear Ru complexes incorporating polypyridyl ligands are particularly interesting and can provide detailed structure information. However, obtaining a single crystal suitable for X-ray crystallography analysis from a diastereomeric mixture is difficult, and only a limited number of X-ray structures of di- and trinuclear ruthenium complexes have been reported.[23]

Therefore, controlling the stereochemistry at the component octahedral metal centers would be of considerable importance, as it would provide only one of the possible diastereomers. Furthermore, the spatial relationship of the components may influence the nature of intramolecular electron- and energy-transfer processes within the assemblies.[24−26] Strategies of controlling the stereochemistry of the octahedral metal centers generally include utilizing the enantiomerically pure building block, such as $[Ru(bpy)_2(py)_2]^{2+}$ or $[Ru(phen)_2(py)_2]^{2+}$,[27−42] and $[Ru(Me_2bpy)_2(CO)_2]^{2+}$;[43,44] the use of chromatographic techniques to isolate the stereoisomers of a number of di- and trinuclear systems;[24,45−51] and using the ligands ("chiragens") which impose a particular stereochemistry on the ultimate products.[52−57]

Herein, we report the syntheses and properties of a series of well-defined homochiral multinuclear Ru complexes based on oligomeric bibenzimidazoles using Λ-$[Ru(bpy)_2(py)_2]$-[(−)-*O*,*O*′-dibenzoyl-L-tartrate]·$12H_2O$ as an enantiomerically pure building block.[34−37,40]

Results and Discussion

Syntheses of Diastereomerically Pure Ru Complexes Based on 2,2′-Bibenzimidazole (1). Mono- and dinuclear Ru complexes represent the simplest examples of the polynuclear assemblies. The studies of the stereoselective

(13) Yin, J.; Elsenbaumer, R. L. *J. Org. Chem.* **2005**, *70*, 9436−9446.
(14) Buckley, A.; Stuetz, D. E.; Serad, G. A. In *Encyclopedia of Polymer Science and Engineering*; Kroschwitz, J. I., Ed.; Wiley: New York, 1988; Vol. 11, pp 572−601.
(15) Haga, M.; Bond, A. M. *Inorg. Chem.* **1991**, *30*, 475−480.
(16) Haga, M.; Matsumura-Inoue, T.; Yamabe, S. *Inorg. Chem.* **1987**, *26*, 4148−4154.
(17) Haga, M.-A. *Inorg. Chim. Acta* **1980**, *45*, L183−L184.
(18) Bond, A. M.; Haga, M. *Inorg. Chem.* **1986**, *25*, 4507−4514.
(19) (a) Haga, M. *Compr. Coord. Chem. II* **2004**, *1*, 125−134. (b) Haga, M.; Ano, T.; Kano, K.; Yamabe, S. *Inorg. Chem.* **1991**, *30*, 3843−3849. (c) Haga, M.-A.; Ali, M. M.; Arakawa, R. *Angew. Chem., Int. Ed. Engl.* **1996**, *35*, 76−78. (d) Haga, M.-A.; Ali, M. M.; Koseki, S.; Fujimoto, K.; Yoshimura, A.; Nozaki, K.; Ohno, T.; Nakajima, K.; Stufkens, D. J. *Inorg. Chem.* **1996**, *35*, 3335−3347. (e) Haga, M.-A.; Ali, M. M.; Maegawa, H.; Nozaki, K.; Yoshimura, A.; Ohno, T. *Coord. Chem. Rev.* **1994**, *132*, 99−104. (f) Haga, M.-A.; Takasugi, T.; Tomie, A.; Ishizuya, M.; Yamada, T.; Hossain, M. D.; Inoue, M. *Dalton Trans.* **2003**, *10*, 2069−2079.
(20) Haga, M. A. *Inorg. Chim. Acta* **1983**, *75*, 29−35.
(21) Rillema, D. P.; Sahai, R.; Matthews, P.; Edwards, A. K.; Shaver, R. J.; Morgan, L. *Inorg. Chem.* **1990**, *29*, 167−175.
(22) Yin, J.; Elsenbaumer, R. L. *Synth. Met.* **2005**, *154*, 233−236.
(23) (a) D'Alessandro, D. M.; Dinolfo, P. H.; Hupp, J. T.; Junk, P. C.; Keene, F. R. *Eur. J. Inorg. Chem.* **2006**, 772−783. (b) Rau, S.; Büttner, T.; Temme, C.; Ruben, M.; Görls, H.; Walther, D.; Duati, M.; Fanni, S.; Vos, J. G. *Inorg. Chem.* **2000**, *39*, 1621−1624. These are representative examples and not the entire crop.
(24) Keene, F. R. *Coord. Chem. Rev.* **1997**, *166*, 121−159.
(25) Keene, F. R. *Coord. Chem. Rev.* **1998**, *27*, 185−194.
(26) von Zelewsky, A. *Stereochemistry of Coordination Compounds*; Wiley: Chichester, 1995.
(27) Bodige, S.; Torres, A. S.; Maloney, D. J.; Tate, D.; Kinsel, G. R.; Walker, A. K.; MacDonnell, F. M. *J. Am. Chem. Soc.* **1997**, *119*, 10364−10369.
(28) Bosnich, B. *Inorg. Chem.* **1968**, *7*, 2379−2386.
(29) Bosnich, B. *Inorg. Chem.* **1968**, *7*, 178−180.
(30) Bosnich, B. *Acc. Chem. Res.* **1969**, *2*, 266−273.
(31) Bosnich, B.; Dwyer, F. P. *Aust. J. Chem.* **1966**, *19*, 2229−2233.
(32) Caspar, R.; Amouri, H.; Gruselle, M.; Cordier, C.; Malézieux, B.; Leveque, H.; Duval, R. *Eur. J. Inorg. Chem.* **2003**, 499−505.
(33) Hiort, C.; Lincoln, P.; Nordén, B. *J. Am. Chem. Soc.* **1993**, *115*, 3448−3454.
(34) Hua, X. Ph.D. Dissertation, University of Fribourg, Switzerland, 1993.
(35) Hua, X.; Lappin, A. G. *Inorg. Chem.* **1995**, *34*, 992−994.
(36) Hua, X.; von Zelewsky, A. *Inorg. Chem.* **1991**, *30*, 3796−3798.
(37) Hua, X.; von Zelewsky, A. *Inorg. Chem.* **1995**, *34*, 5791−5797.
(38) Kolp, B.; Viebrock, H.; von Zelewsky, A.; Abeln, D. *Inorg. Chem.* **2001**, *40*, 1196−1198.
(39) MacDonnell, F. M.; Bodige, S. *Inorg. Chem.* **1996**, *35*, 5758−5759.
(40) Morgan, O.; Wang, S.; Bae, S.-A.; Morgan, R. J.; Baker, A. D.; Strekas, T. C.; Engel, R. *J. Chem. Soc., Dalton Trans.* **1997**, 3773−3776.
(41) Tzalis, D.; Tor, Y. *J. Am. Chem. Soc.* **1997**, *119*, 852−853.
(42) Wärnmark, K.; Thomas, J. A.; Heyke, O.; Lehn, J.-M. *Chem. Commun.* **1996**, 701−702.
(43) Rutherford, T. J.; Pellegrini, P. A.; Aldrich-Wright, J.; Junk, P. C.; Keene, F. R. *Eur. J. Inorg. Chem.* **1998**, 1677−1688.
(44) Rutherford, T. J.; Quagliotto, M. G.; Keene, F. R. *Inorg. Chem.* **1995**, *34*, 3857−3858.
(45) Fletcher, N. C.; Junk, P. C.; Reitsma, D. A.; Keene, F. R. *J. Chem. Soc., Dalton Trans.* **1998**, 133−138.
(46) Kelso, L. S.; Reitsma, D. A.; Keene, F. R. *Inorg. Chem.* **1996**, *35*, 5144−5153.
(47) Patterson, B. T.; Keene, F. R. *Inorg. Chem.* **1998**, *37*, 645−650.
(48) Reitsma, D. A.; Keene, F. R. *J. Chem. Soc., Dalton Trans.* **1993**, 2859−2860.
(49) Rutherford, T. J.; Keene, F. R. *Inorg. Chem.* **1997**, *36*, 3580−3581.
(50) Rutherford, T. J.; Keene, F. R. *J. Chem. Soc., Dalton Trans.* **1998**, 1155−1162.
(51) Rutherford, T. J.; Van Gijte, O.; Kirsch-De Mesmaeker, A. e.; Keene, F. R. *Inorg. Chem.* **1997**, *36*, 4465−4474.
(52) Fletcher, N. C.; Keene, F. R.; Viebrock, H.; von Zelewsky, A. *Inorg. Chem.* **1997**, *36*, 1113−1121.
(53) Hamann, C.; von Zelewsky, A.; Neels, A.; Stoeckli-Evans, H. *Dalton Trans.* **2004**, 402−406.
(54) Mamula, O.; von Zelewsky, A. *Coord. Chem. Rev.* **2003**, *242*, 87−95.
(55) Mamula, O.; von Zelewsky, A.; Brodard, P.; Schläpfer, C.-W.; Bernardinelli, G.; Stoeckli-Evans, H. *Chem. Eur. J.* **2005**, *11*, 3049−3057.
(56) Mürner, H.; Belser, P.; von Zelewsky, A. *J. Am. Chem. Soc.* **1996**, *118*, 7989−7994.
(57) von Zelewsky, A. *Coord. Chem. Rev.* **1999**, *190−192*, 811−825.

Scheme 1. Synthesis of Λ-[Ru(bpy)$_2$(BiBzImH$_2$)](PF$_6$)$_2$ (Λ-**3**)

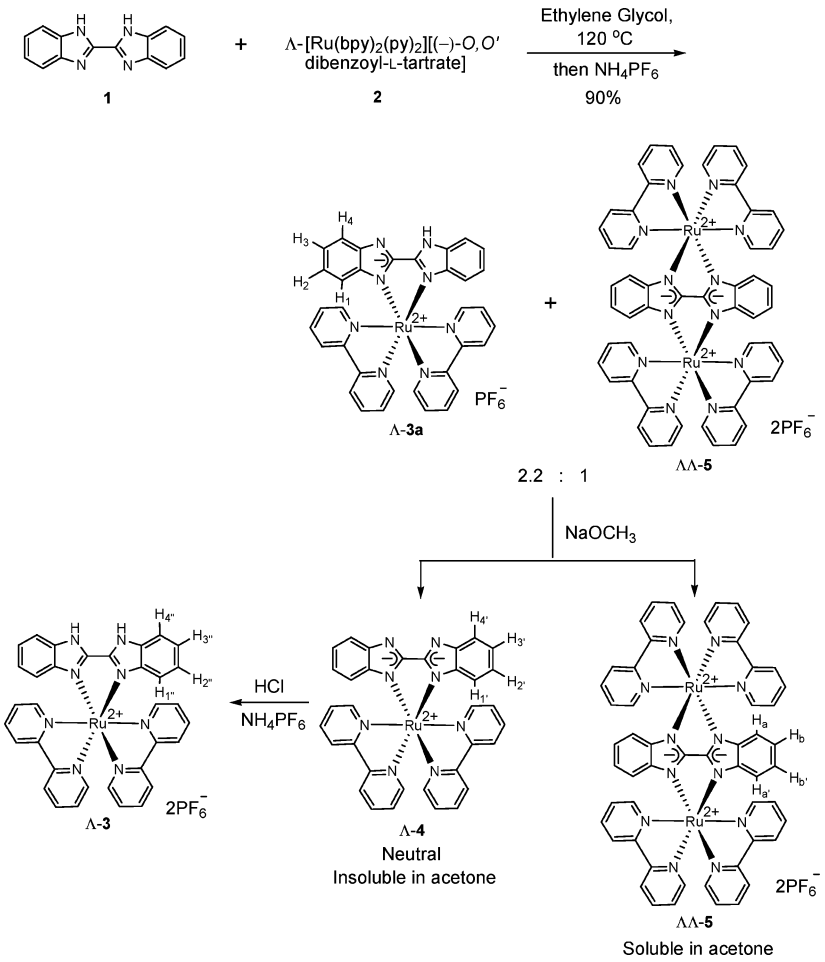

synthesis of individual enantiomeric or diastereoisomeric forms or the separation of these individual stereoisomeric forms from a mixture would provide useful information for the characterization of the complexes with higher nuclearity. To probe the stereochemical control in the polynuclear assemblies of the oligomeric bibenzimidazoles, our study started with the synthesis of the enantiomerically pure mono-Ru complex Λ-**3** (Scheme 1).

Λ-[Ru(bpy)$_2$(py)$_2$][(−)-*O*,*O*′-dibenzoyl-L-tartrate]·12H$_2$O (**2**) was reacted with an excess of 2,2′-bibenzimidazole (**1**) in ethylene glycol at 120 °C. The reactions were carried out in the absence of light as a precaution of photoracemization. This applied to all the complexation reactions throughout the paper. Interestingly, two complexes were obtained, which were shown to be the mono-deprotonated complex Λ-**3a** and the bis-Ru complex ΛΛ-**5** (2.2:1), by NMR spectroscopy and a further control experiment (Scheme 1 and Figure 1).

The formation of Λ-**3a** is due to the deprotonation of Λ-**3** by pyridine released from the enantiopure building block **2**. The acidity of the bibenzimidazole ligand increases upon the coordination with the ruthenium ion, rendering facile deprotonation of the complex Λ-**3**. The pK_a values of [Ru(bpy)$_2$(BiBzImH$_2$)]$^{2+}$ in a 50% acetonitrile/water mixture have been reported: pK_{a1} and pK_{a2} are equal to 5.74 ± 0.05 and 10.51 ± 0.05 at 25 °C, respectively.[15−18,20] The pK_a of pyridinium ion is 5.25, which means that pyridine is basic enough to deprotonate the formed model complex Λ-**3**, rendering the formation of Λ-**3a**, which was further complexed to provide the bis-Ru complex ΛΛ-**5**.

The mixture of the mono-deprotonated Λ-**3a** and the bis-Ru complex ΛΛ-**5** was separated after deprotonation with NaOCH$_3$. Λ-**3a** was fully deprotonated to give the complex Λ-**4**, which was not soluble in acetone. The bis-Ru complex ΛΛ-**5** was stable, remaining unchanged under the basic condition, and its PF_6^- salt was soluble in acetone. Therefore, Λ-**4** was separated from ΛΛ-**5** by simple filtration. Then, the pure deprotonated Λ-**4** was protonated by HCl to give the pure protonated model compound Λ-**3**. The structures of the products were confirmed by the NMR study (Figure 1). The protons H$_1$/H$_{1'}$/H$_{1''}$ and H$_a$/H$_{a'}$ are on the bibenzimidazole ligand, which are in the shielding zone of the aromatic ring of the bpy; therefore, they are strongly upfield shifted ($\delta = 5-6$). The structure of the bis-Ru complex ΛΛ-**5** was further confirmed by the control experiment shown in Scheme 2: it was obtained by the reaction of **1** with 2.1 equiv of the enantiopure building block **2**.

Compared to the stereoselective synthesis, the synthesis of the racemic mono-Ru complex [Ru(bpy)$_2$(BiBzImH$_2$)]$^{2+}$ (**3**) by complexing **1** with Ru(bpy)$_2$Cl$_2$ gave the desired complex **3** without deprotonation, along with a small

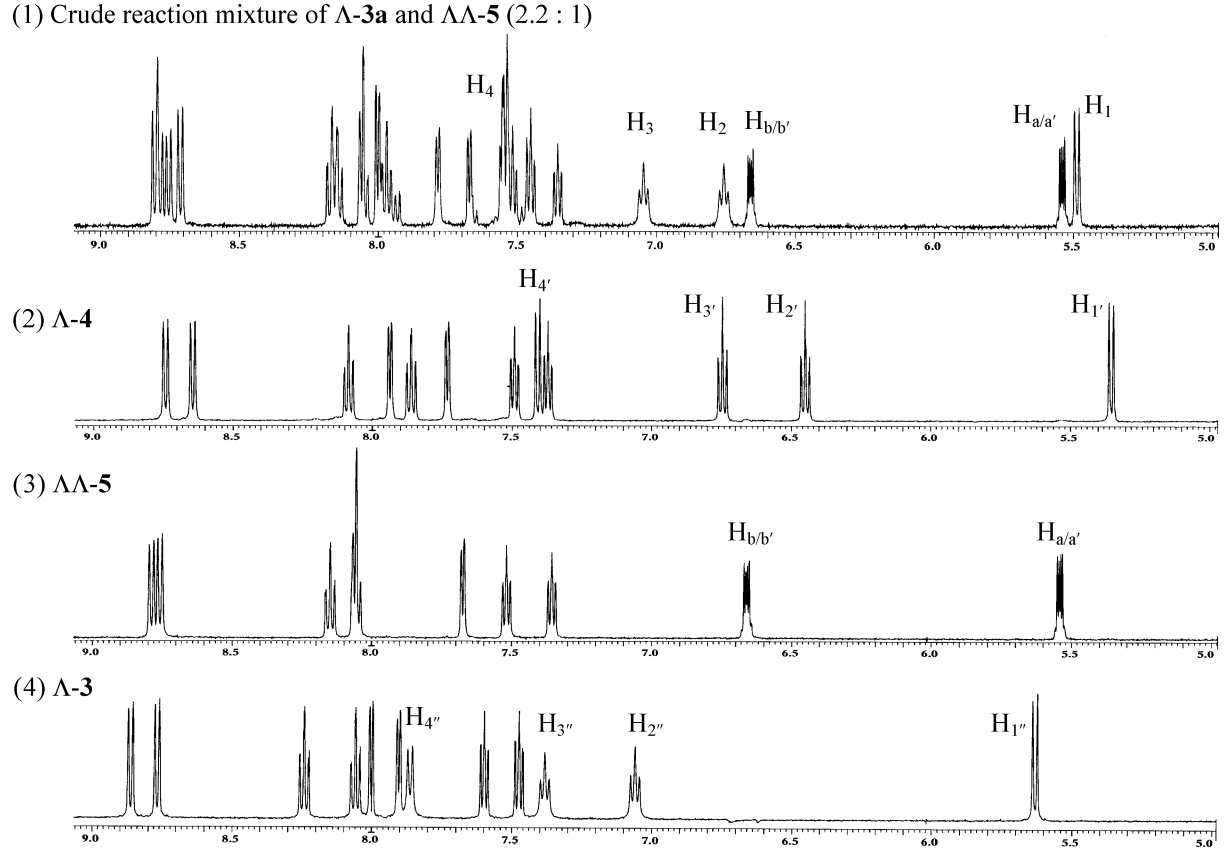

Figure 1. ^{1}H NMR spectra of the chiral Ru complexes in Scheme 1. (1) Crude reaction mixture: Λ-**3a** and ΛΛ-**5** (2.2:1). (2) Λ-**4**, $H_{1'}$, $H_{2'}$, $H_{3'}$, $H_{4'}$ are upfield-shifted compared to H_1, H_2, H_3, H_4. (3) ΛΛ-**5**. $H_{a/a'}$, $H_{b/b'}$ remained unchanged after the base treatment. (4) Λ-**3**, $H_{1''}$, $H_{2''}$, $H_{3''}$, $H_{4''}$ are downfield-shifted compared to $H_{1'}$, $H_{2'}$, $H_{3'}$, $H_{4'}$. (Concentrations of the above Ru complexes in DMSO-d_6 are approximately the following values: (1) Λ-**3a**, 2.95 M. ΛΛ-**5**, 1.34 M. (2) Λ-**4**, 4.30 M. (3) ΛΛ-**5**, 2.00 M. (4) Λ-**3**, 3.60 M.)

Scheme 2. Synthesis of ΛΛ-**5** and *rac*-**3**

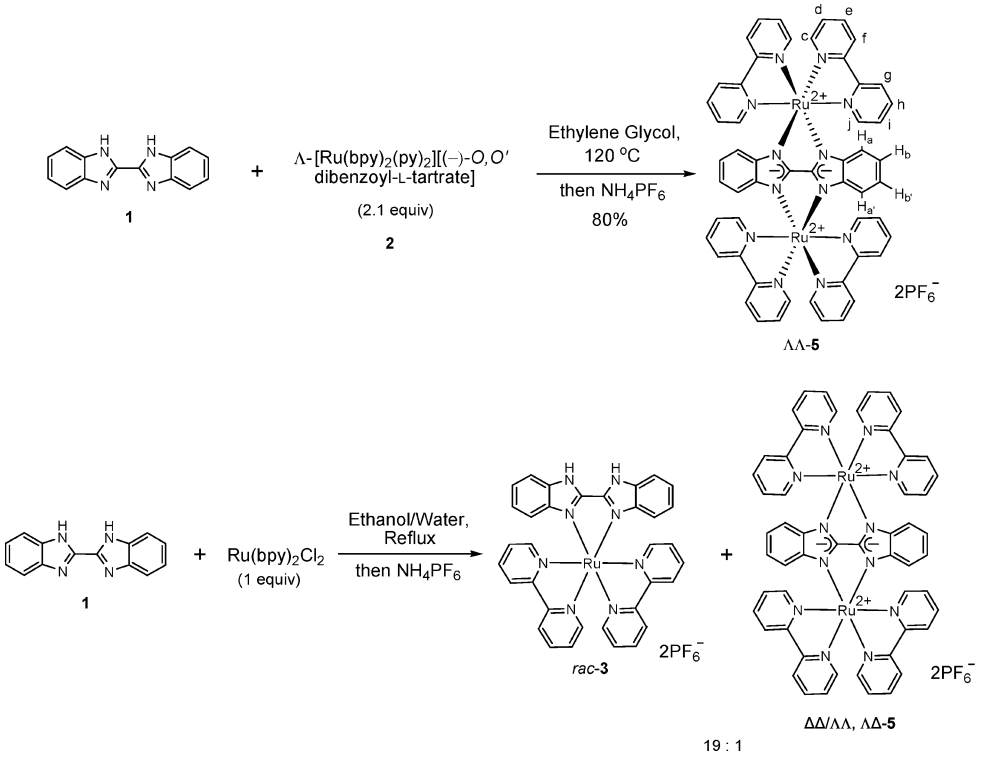

amount of the dinuclear complex **5** in a ratio of 19:1 (Scheme 2).

Optical Purity of ΛΛ-[Ru(bpy)$_2$(BiBzIm)Ru(bpy)$_2$](PF$_6$)$_2$ (ΛΛ-5). The ^{1}H NMR spectra of ΛΛ-**5** prepared from

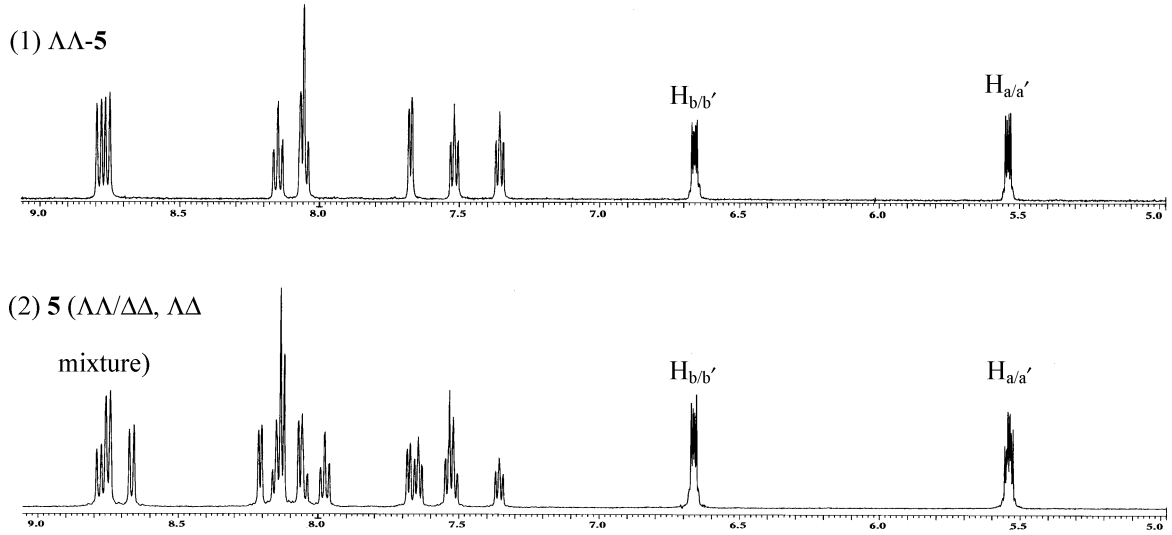

Figure 2. ^{1}H NMR spectra of $[Ru(bpy)_2(BiBzIm)Ru(bpy)_2](PF_6)_2$. (1) ΛΛ-**5**. (2) **5** prepared from $Ru(bpy)_2Cl_2$.

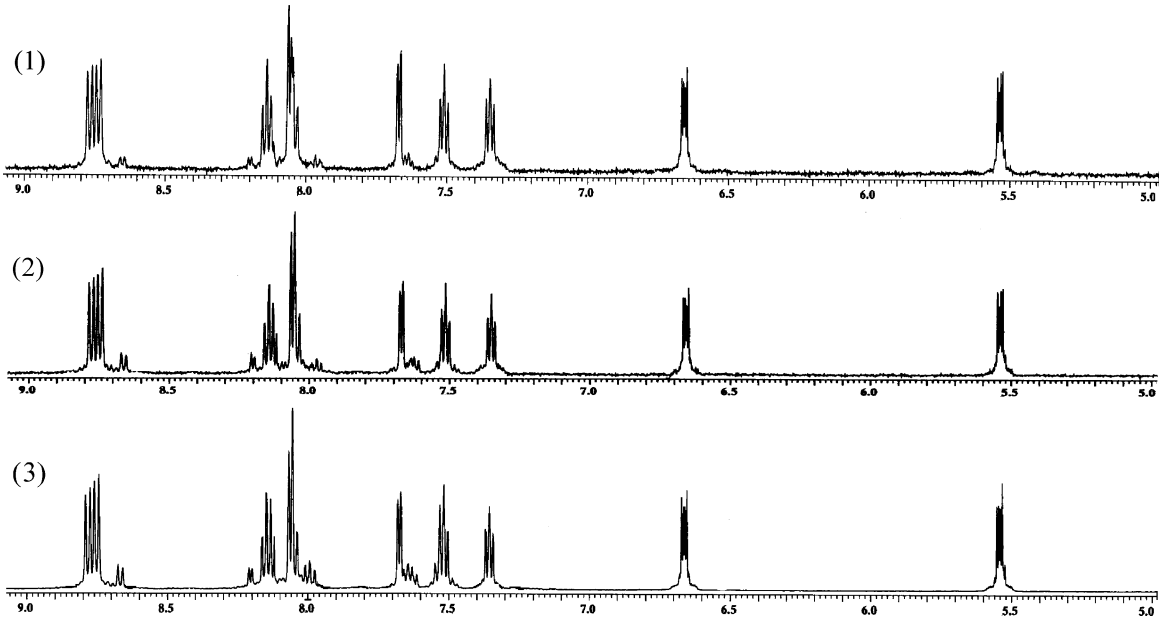

Figure 3. NMR studies on the racemization of the synthesis of ΛΛ-$[Ru(bpy)_2(BiBzIm)Ru(bpy)_2](PF_6)_2$ (ΛΛ-**5**). (1) 120 °C 8 h, 3% racemized. (2) 120 °C 22 h, 6% racemized. (3) 120 °C 50 h, 10% racemized.

the enantiopure building block **2** and **5** prepared from $Ru(bpy)_2Cl_2$ are different, as shown in Figure 2, which provided an accurate and definite method for the determination of diastereomeric purity of ΛΛ-**5** synthesized under a variety of conditions described below. The D_2 symmetry of ΛΛ-**5** requires the equivalence of the four bpy ligands. A total of 10 magnetically nonequivalent protons is therefore observed (spectrum 1 in Figure 2). $H_{a/a'}$ and $H_{b/b'}$ are the protons on the bibenzimidazole bridging ligand. $H_{a/a'}$ lie in the shielding zone of the adjacent bpy rings ($\delta = 5.5$). The rest of eight proton signals representing protons c−j on the bpy ligand. The ^{13}C NMR spectra of ΛΛ-$[Ru(bpy)_2(BiBzIm)Ru(bpy)_2](PF_6)_2$ gives 14 lines (10 lines from ligand bpy and 4 lines from BiBzIm) (Supporting Information). With the use of the racemic $Ru(bpy)_2Cl_2$, the diastereoisomers (ΔΔ/ΛΛ and ΔΛ) were obtained (spectrum 2 in Figure 2). The relative abundance of the meso form and the enantiomeric pair is around 55:45.

The degree of stereoretention in the formation of ΛΛ-**5** was studied under a variety of conditions, as given in Table 1. The isomerization occurs at elevated temperatures and with extended reaction times. All reactions were observed to proceed with near-complete retention of configuration, whereas racemization occurred to varying degrees for all complexes at elevated temperatures.[43,44,58] The PF_6^- salt was not purified either by column separation or by ether precipitation to provide the real value of the percentage of the racemization.

There are two likely stages at which the racemization might occur: the enantiopure building block (**2**) racemized

(58) Rutherford, T. J.; Reitsma, D. A.; Keene, F. R. *J. Chem. Soc., Dalton Trans.* **1994**, 3659−3666.

Table 1. Study of Racemization on the Formation of ΛΛ-[Ru(bpy)$_2$(BiBzIm)Ru(bpy)$_2$](PF$_6$)$_2$ (ΛΛ-**5**)[a]

reaction conditions	percentage of racemization
100 °C, 8 h	2%, with 17% enantiopure building block unreacted
100−110 °C, 20 h	3%
100−115 °C, 50 h	8%
120 °C, 8 h	3%
120 °C, 22 h	6%
120 °C, 50 h	10%
165 °C, 4 h	15%
165 °C, 8 h	16%
165 °C, 22 h	18%

[a] Solvent: ethylene glycol.

before being complexed with bibenzimidazole (**1**) or the product ΛΛ-**5** racemized under extensive heating. A further control experiment was carried out to demonstrate that the enantiopure building block (**2**) racemized under heating before complexation with ligand **1**: the enantiopure building block (**2**) was first heated at 120 °C for 5 h, then reacted with an optically active bidentate ligand (1*R*,2*R*)-(−)-1,2-diaminocyclohexane (*R*,*R*-dach) for 4 h.[37] The obtained products were a pair of diastereomers Λ-[Ru(bpy)$_2$(*R*,*R*-dach)]$^{2+}$ and Δ-[Ru(bpy)$_2$(*R*,*R*-dach)]$^{2+}$ with an approximate 1:1.25 ratio on the basis of the ^{1}H NMR study, which indicates that the enantiopure building block racemized into Δ-[Ru(bpy)$_2$(py)$_2$]$^{2+}$ and Λ-[Ru(bpy)$_2$(py)$_2$]$^{2+}$ before it was complexed with *R*,*R*-dach.

The other likely stage of racemization occurs with extended heating time, as shown in Table 1.

On the basis of the above model study, the synthesis of ΛΛ-**5** at 120 °C for 8 h would be appropriate due to the low value of racemization and the short reaction time. The tetra-Ru and octa-Ru complexes were synthesized under the same condition to minimize the racemization as described below.

Synthesis of Λ$_4$-[(Ru(bpy)$_2$)$_4$(bis(BiBzIm))](PF$_6$)$_4$ (Λ$_4$-Ru$_4$-6). The homochiral tetra-Ru complex Λ$_4$-[(Ru(bpy)$_2$)$_4$(bis(BiBzIm))](PF$_6$)$_4$ (Λ$_4$-Ru$_4$-**6**) was synthesized by the complexation of bis-bibenzimidazole (**7**) with an excess of the enantiopure building block (**2**) (i.e., 4.4 equiv) to ensure full complexation (Scheme 3). On the basis of the model study of bis-Ru complex ΛΛ-**5**, 3% racemized when the reaction was carried out at 120 °C for 8 h. The tetra-Ru complex obtained under the same reaction conditions could be around 6% racemized. The formation of the tetra-Ru complex Λ$_4$-Ru$_4$-**6** was confirmed by matrix-assisted laser desorption ionization (MALDI-TOF) mass spectrometry (Figure 4) and the satisfactory elemental analysis. The mass spectrum clearly shows the parent ion complex minus 1PF$_6^-$, 2PF$_6^-$, 3PF$_6^-$, and 4PF$_6^-$ fragments.

X-ray Crystallography. A limited number of crystal structures of dinuclear ruthenium complexes incorporating polypyridyl ligands have been reported.[23] The crystal structures of higher nuclearity polymetallic assemblies are relatively scarce. The single crystals of the PF$_6^-$ salt of Λ$_4$-Ru$_4$-**6** were grown from the acetone/water solution by the slow evaporation. They were composed of very small weak scattering crystals, crumbling easily and being extremely

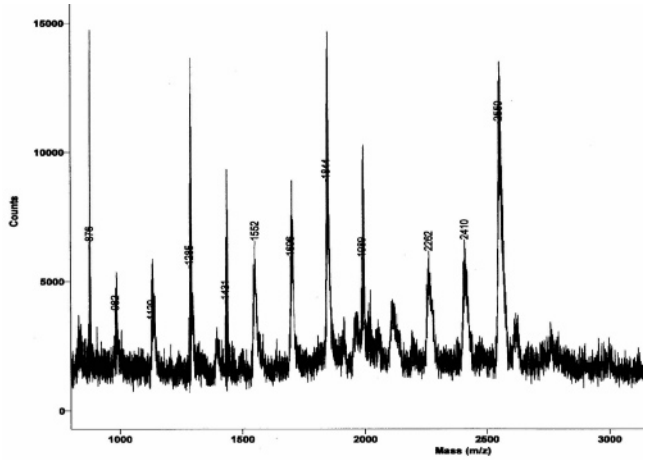

Figure 4. MALDI-TOF spectra of Λ$_4$-[(Ru(bpy)$_2$)$_4$(bis(BiBzIm))](PF$_6$)$_4$ (Λ$_4$-Ru$_4$-**6**). 2550 [M − 1PF$_6$]$^+$, 2410 [M − 2PF$_6$]$^+$, 2262 [M − 3PF$_6$]$^+$, 2116 [M − 4PF$_6$]$^+$.

Scheme 3. Synthesis of Λ$_4$-[(Ru(bpy)$_2$)$_4$(bis(BiBzIm))](PF$_6$)$_4$ (Λ$_4$-Ru$_4$-**6**)

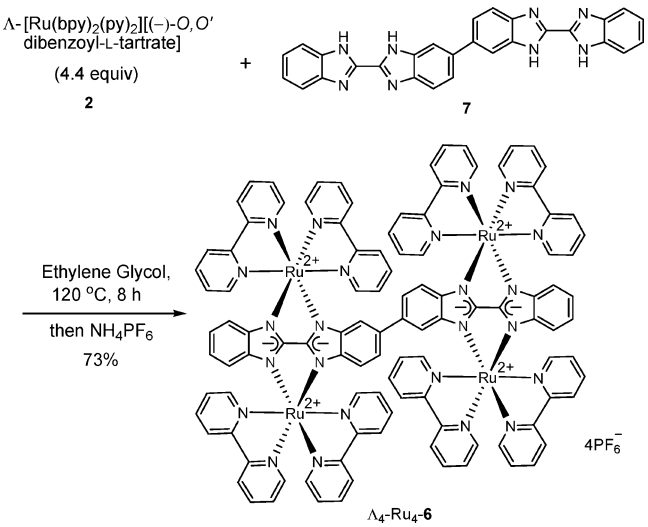

prone to solvent evaporation. The structure was solved, which is the refined single-crystal structure of the highest nuclearity multinuclear Ru complex up to date. Λ$_4$-[(Ru(bpy)$_2$)$_4$(bis(BiBzIm))](PF$_6$)$_4$ crystallized in the monoclinic space group $P2_1$. A perspective view of the crystal structure is shown in Figure 5, and details of the bond lengths and angles are provided in Tables S1−S3 (Supporting Information). The proof of an enantiopure crystal structure was given from the Flack absolute structure parameter, which is 0.00(3). (The scale factor for the inversion twin refinement is (−100, 1−10, 00−1).) All four Ru centers have Λ octahedral configurations, with a Ru−Ru separation of 5.509 Å across the bibenzimidazole ligand. The bridging ligand bis-bibenzimidazole remained nearly coplanar after complexation with four Ru(bpy)$_2$ units, which is good for the electron delocalization between the two bibenzimidazole repeat units.

Synthesis of Λ$_8$-[(Ru(bpy)$_2$)$_8$(tetra(BiBzIm))](PF$_6$)$_8$ (Λ$_8$-Ru$_8$-8). The same strategy was applied for the synthesis of the homochiral octa-Ru complex Λ$_8$-Ru$_8$-**8** using the ligand tetra-bibenzimidazole (**9**) (Scheme 4). An excess of the enantiopure building block (**2**) (8.4 equiv) was added to ensure the full deprotonation and complexation of the

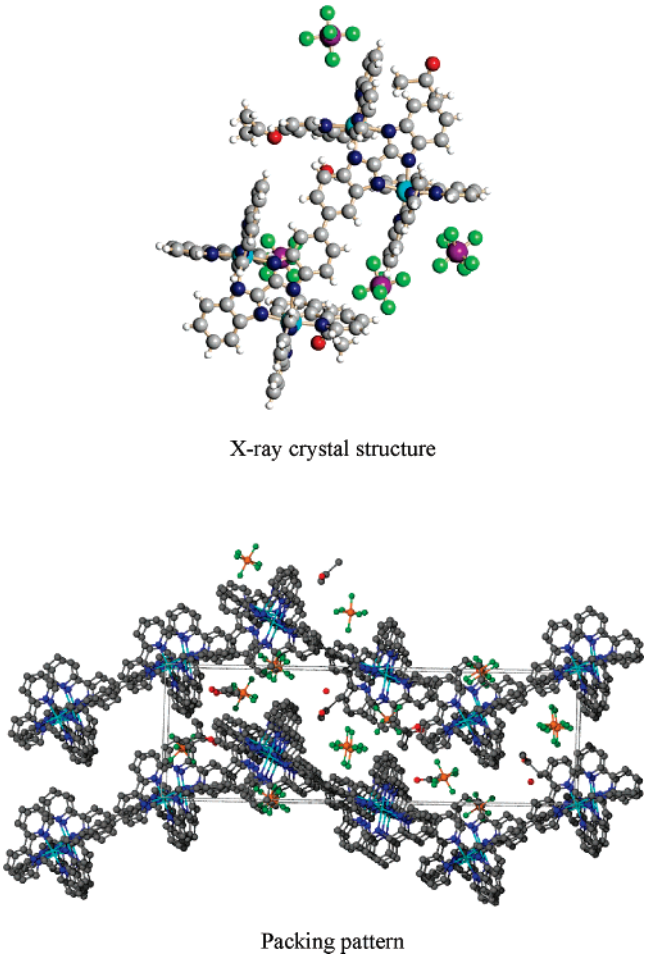

Figure 5. X-ray structure and packing pattern of Λ_4-[(Ru(bpy)$_2$)$_4$(bis-(BiBzIm))](PF$_6$)$_4$ (Λ_4-Ru$_4$-**6**). (Grown from acetone/water solution.)

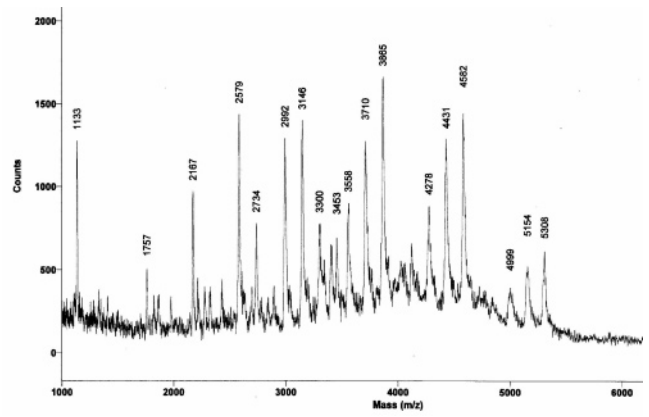

Figure 6. MALDI-TOF spectra of Λ_8-[(Ru(bpy)$_2$)$_8$(tetra(BiBzIm))](PF$_6$)$_8$ (Λ_8-Ru$_8$-**8**). 5308 [M − 1PF$_6$]$^+$, 5154 [M − 2PF$_6$]$^+$, 4999 [M − 3PF$_6$]$^+$, 4582 [M − 6PF$_6$]$^+$, 4431 [M − 7PF$_6$]$^+$, 4278 [M − 8PF$_6$]$^+$.

tetramer ligand **9**. If the reaction was carried out at 120 °C, then the yield of the octa-Ru complex was very low (around 10%) due to the low solubility of the ligand **9**. If the reaction was carried out at 150−160 °C, then the yield was 55%, but around 64% racemization could occur, according to the model study shown in Table 1. In addition, the circular dichroism (CD) spectra of Λ_8-Ru$_8$-**8** obtained from the reaction carried out at 150 °C for 15 h show a lower

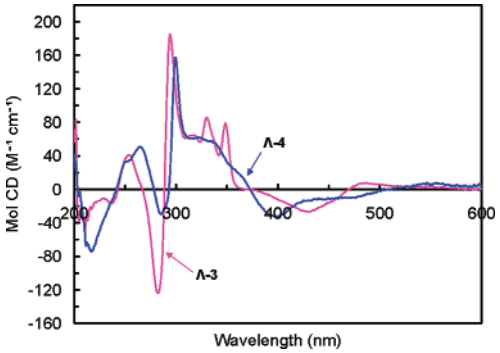

Figure 7. Circular dichroism spectra of Λ-[Ru(bpy)$_2$(BiBzImH$_2$)](PF$_6$)$_2$ (Λ-**3**) and Λ-[Ru(bpy)$_2$(BiBzIm)] (Λ-**4**) in acetonitrile. (The concentrations of the Ru complexes are around 1.36 × 10^{-5} M.)

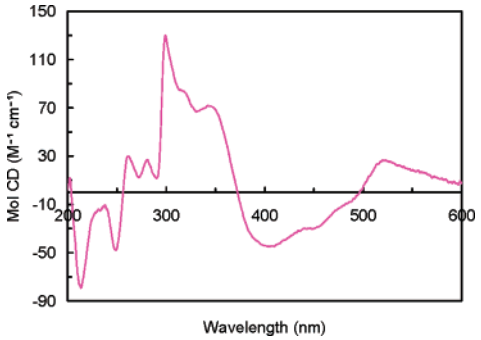

Figure 8. Circular dichroism spectra of ΛΛ-[Ru(bpy)$_2$(BiBzIm)$_2$Ru(bpy)$_2$]-(PF$_6$)$_2$ (ΛΛ-**5**) in acetonitrile. (The concentration of the Ru complex is around 1.70 × 10^{-5} M.)

amplitude than that of the tetra-Ru complex, which indicates that there was more racemization that occurred than with the synthesis of the tetra-Ru complex.

The formation of the octa-Ru complex Λ_8-Ru$_8$-**8** was confirmed by the MALDI-TOF analysis (Figure 6). The spectrum clearly shows the parent ion complex minus 1PF$_6^-$, 2PF$_6^-$, ... , 7PF$_6^-$, and 8PF$_6^-$ fragments.

Absolute Configuration. The CD spectra of the homochiral Ru complexes are shown in Figures 7−10. The Cotton effects are observed and are in agreement with the expected Λ absolute configurations,[28−31] i.e., under the long-axis-polarized band around 294 nm, the circular dichroism is at low energies strongly positive, at higher energies negative, and positive at the lowest energy MLCT transition. Therefore, the substitution of the pyridine ligands proceeds with the retention of configuration.

UV−Vis Properties. The UV−vis absorption data of the homochiral Ru complexes are shown in Table 2. The UV−vis spectra of ΛΛ-**5**, Λ_4-Ru$_4$-**6**, and Λ_8-Ru$_8$-**8** are overlaid in Figure 11. For ΛΛ-**5**, the low-energy transition at 506 nm is assigned as dπ−π* (bpy) metal-to-ligand charge-transfer (MLCT) transitions. The spectral activity in the 350 nm region consists of the BiBzIm-based intraligand π−π* transition overlapped with the MLCT bands. The absorption maximum at 294 nm has its primary origin of π−π* (bpy) transitions. The far UV transitions increase in a systematic manner as the number of heterocyclic ligands increases and most likely are overlapping π−π* transitions associated with both bpy and BiBzImH$_2$ ligands.[16,20,21]

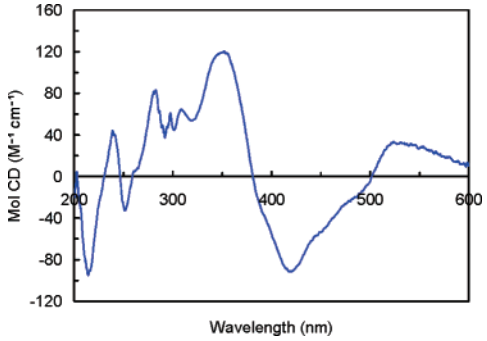

Figure 9. Circular dichroism spectra of Λ_4-[(Ru(bpy)$_2$)$_4$(bis(BiBzIm))](PF$_6$)$_4$ (Λ_4-Ru$_4$-**6**) in acetonitrile. (The concentration of the Ru complex is around 1.33×10^{-5} M.)

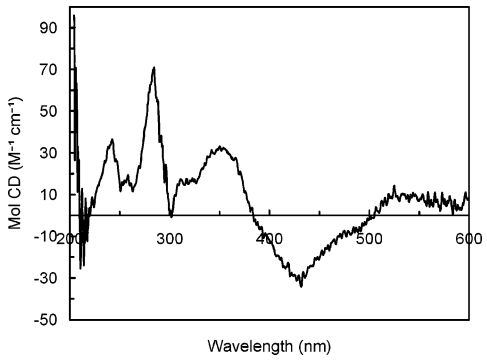

Figure 10. Circular dichroism spectra of Λ_8-[(Ru(bpy)$_2$)$_8$(tetra(BiBzIm))](PF$_6$)$_8$ (Λ_8-Ru$_8$-**8**) in acetonitrile. (The concentration of the Ru complex is around 5.86×10^{-6} M.)

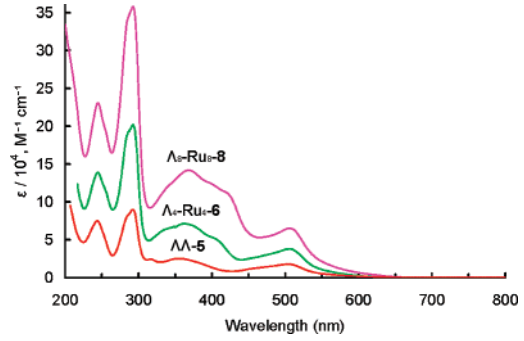

Figure 11. UV−vis spectra of bis-Ru complex [(Ru(bpy)$_2$)$_2$(BiBzIm)](PF$_6$)$_2$ ($\Lambda\Lambda$-**5**), tetra-Ru complex [(Ru(bpy)$_2$)$_4$(bis(BiBzIm))](PF$_6$)$_4$ (Λ_4-Ru$_4$-**6**), and octa-Ru complex [(Ru(bpy)$_2$)$_8$(tetra(BiBzIm))](PF$_6$)$_8$ (Λ_8-Ru$_8$-**8**) in CH_3CN.

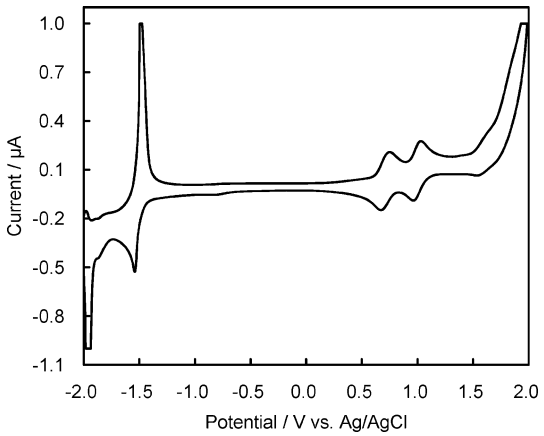

Figure 12. Cyclic voltammogram of octa-Ru complex [(Ru(bpy)$_2$)$_8$(tetra(BiBzIm))](PF$_6$)$_8$ (Λ_8-Ru$_8$-**8**) in 0.10 M [(n-C_4H_9)$_4$N]PF$_6$/CH_3CN solution at a scan rate of 50 mV·s^{-1} . The concentration of the Ru complex is around 2.11×10^{-4} M.

For the tetranuclear complex Λ_4-Ru$_4$-**6**, the band at 363 nm consists of the bis(BiBzIm)-based $\pi-\pi^*$ transition overlapped with the multiple MLCT bands. The lowest energy MLCT absorption (506 nm) is at the same position as the MLCT of the dinuclear complex $\Lambda\Lambda$-**5**, and the peak molar extinction coefficient is around double that of $\Lambda\Lambda$-**5**, which is the approximate additive relationship of the number of the independent chromophores between the tetra-Ru and bis-Ru complex. The extension of the bridging ligand from the monomer (**1**) to the dimer of bibenzimidazole (**7**) does not change the position of the lowest energy MLCT transition, which is still d$\pi-\pi^*$ (bpy) in nature.

The UV−vis spectrum of the octa-Ru complex Λ_8-Ru$_8$-**8** is very similar to the tetra-Ru complex Λ_4-Ru$_4$-**6**. The extinction coefficient is approximately double that of the tetra-Ru complex Λ_4-Ru$_4$-**6**. The lowest energy MLCT transition remains at 506 nm (ϵ = 70 200 M^{-1}·cm^{-1}). The

Scheme 4. Synthesis of Λ_8-[(Ru(bpy)$_2$)$_8$(tetra(BiBzIm))](PF$_6$)$_8$ (Λ_8-Ru$_8$-**8**)

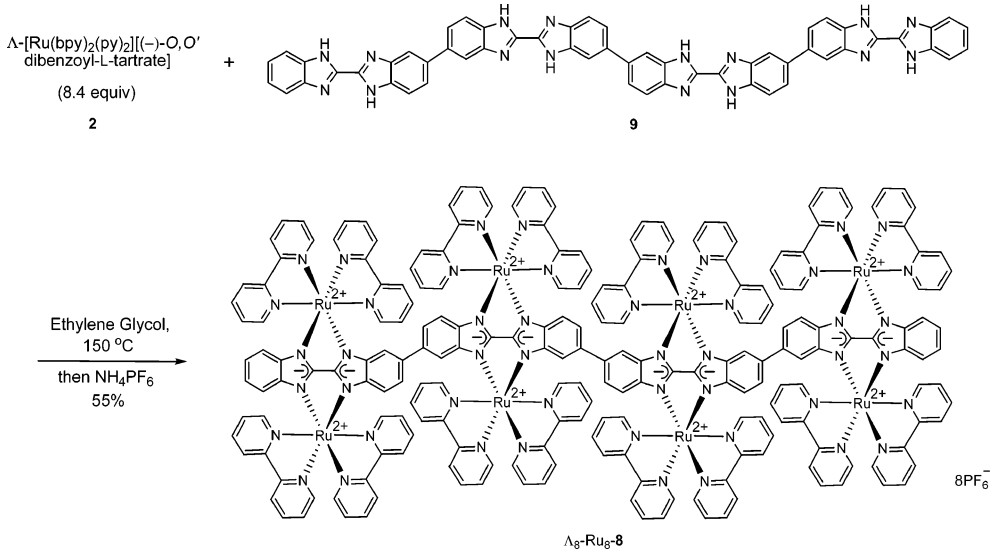

Table 2. UV−vis Absorption Spectral Data for Ru Complexes Based on Bibenzimidazole Oligomers in CH_3CN at 298 K (λ, nm (ϵ, $M^{-1}\cdot cm^{-1}$))

Ru complex	$\pi-\pi^*$ (bpy)		$\pi-\pi^*$ (oligomeric $BiBzImH_2$/BiBzIm overlapped with MLCT)		$d\pi-\pi^*$ (bpy)
$[Ru(bpy)_2(BiBzImH_2)]^{2+}$ (**Λ-3**)[a,b]	240 (39 400)	290 (63 100)	328 (37 500)	347 (45 800)	469 (11 300) 438 (sh)
$[Ru(bpy)_2(BiBzIm)]$ (**Λ-4**)[a]	243 (55 100)	295 (54 700)	333 (30 400)		543 (8470)
$[(Ru(bpy)_2)_2(BiBzIm)]^{2+}$ (**ΛΛ-5**)[b]	244 (80 300)	294 (104 000)	318 (25 600)	355 (27 000)	506 (19 500)
$[(Ru(bpy)_2)_4(bis\text{-}BiBzIm)]^{4+}$ (Λ_4-Ru_4-**6**)	244 (141 000)	293 (212 000)	363 (73 100) 333 (sh)	398 (sh)	506 (38 000)
$[(Ru(bpy)_2)_8(tetra\text{-}BiBzIm)]^{8+}$ (Λ_8-Ru_8-**8**)	244 (243 000)	292 (382 000)	367 (147 000)	415 (sh) (118 000)	505 (70 200)

[a] Reference 20. [b] References 16 and 21.

Table 3. Cyclic Voltammogram Data for Ru Complexes Based on Bibenzimidazole Oligomers[a]

Ru complex	oxidation		reduction	
	$E_{1/2}$ (1), (V)	$E_{1/2}$ (2), (V)	$E_{1/2}'$ (1), (V)	$E_{1/2}'$ (2), (V)
$[Ru(bpy)_2(BiBzImH_2)]^{2+}$ [b] (**Λ-3**)	1.12 (70)		−1.60 (80)	−1.90 (80)
$[Ru(bpy)_2(BiBzIm)]$[b] (**Λ-4**)	0.43 (68)		−1.58 (60)	−1.87 (60)
$[(Ru(bpy)_2)_2(BiBzIm)]^{2+}$[b,c] (**ΛΛ-5**)	0.76 (60)	1.04 (64)	−1.54 (100)[d]	−1.82 (120)[d]
$[(Ru(bpy)_2)_4(bis\text{-}BiBzIm)]^{4+}$ (Λ_4-Ru_4-**6**)	0.75 (81)	1.04 (72)	−1.47 (124)	−1.64 (443)
$[(Ru(bpy)_2)_8(tetra\text{-}BiBzIm)]^{8+}$ (Λ_8-Ru_8-**8**)	0.71 (78)	1.00 (69)	−1.51 (55)	−1.72 (473)

[a] Solutions are 0.1 M $[(n\text{-}C_4H_9)_4N]PF_6$ in acetonitrile. The potentials $E_{1/2}$ were calculated from the equation $(E_{pa} + E_{pc})/2$ where E_{pa} and E_{pc} are anodic and cathodic peak potentials, respectively. The values in parentheses are peak-to-peak separations, $\Delta E_p = E_{pa} - E_{pc}$. [b] Reference 20. [c] References 16 and 21. [d] This work.

π^* of the bpy could be lower than π^* of the tetra-$BiBzImH_2$, therefore, the lowest energy MLCT transition is $d\pi-\pi^*$ (bpy) in nature. The progressive lowering of the π^* orbitals of the bridging ligands from the dimer to the tetramer of bibenzimidazole does not change the position of the lowest energy MLCT transition. This indicates that the extension of the conjugated chain lengths of the bridging ligands does not provide the pathway for the electronic communication between the metal centers.

Electrochemical Properties. The cyclic voltammogram (CV) of the tetranuclear Ru complex (Λ_4-Ru_4-**6**) exhibits two oxidation waves at +0.75 and +1.04 V (Table 3). These occur at the same potentials as the nonchiral tetra-Ru complex **6** we reported previously.[22] They are close to the oxidation potentials +0.77 and +1.06 V of the dinuclear complex ΛΛ-**5**. The separations between the anodic and cathodic peak potentials, ΔE_p, are 81 and 72 mV, respectively; the ratios of the oxidation to the reduction peak heights are 1.0, which indicates that the oxidation processes are quasi-reversible. Four one-electron steps are involved in these two oxidation processes. The redox properties indicate that any electronic interaction between the Ru metals along the conjugated **7** is weak.

It has been shown that the first oxidation potential of the dinuclear Ru complex ΛΛ-**5** is 0.3 V lower than that of the mononuclear complex Λ-**3**, which indicates that the BiBzIm bridging ligand in the dinuclear complex ΛΛ-**5** has an electron-donor property. The tetranuclear complex Λ_4-Ru_4-**6** has the same oxidation behavior as the dinuclear complex ΛΛ-**5**, which suggests that the dimer of BiBzIm (**7**) also has an electron-donor property. The Ru−Ru electrostatic interactions across the bridging ligand **7** are similar to the Ru−Ru interaction in the dinuclear complex ΛΛ-**5**.

The tetranuclear complex Λ_4-Ru_4-**6** exhibits reduction potentials at −1.47 and −1.64 V. The sharp spikes might be due to the adsorption on the electrode. They may be the bpy ligand-based processes according to the previous results. The ΔE_p spacings (124 and 443 mV) and the increased currents suggest that more than one single electron-transfer step occurs at each wave. This is reasonable given the presence of more than one $Ru(bpy)_2^{2+}$ unit.

The CV of the octanuclear Ru complex (Λ_8-Ru_8-**8**) is shown in Figure 12. It exhibits two oxidation waves at +0.71 and +1.00 V. They are close to the two oxidation potentials +0.77 and +1.06 V of the dinuclear complex ΛΛ-**5**. Λ_8-Ru_8-**8** still undergoes the bpy-based reduction at −1.51 and −1.72 V. The Ru−Ru electrostatic interactions across the bridging ligand **9** is similar to the Ru−Ru interactions in the dinuclear and the tetranuclear complexes ΛΛ-**5** and Λ_4-Ru_4-**6**. However, interactions along the tetra-bibenzimidazole ligand are relatively weak.

Conclusions

The homochiral multinuclear Ru complexes of the oligomeric bibenzimidazoles were synthesized stereoselectively using Λ-$[Ru(bpy)_2(py)_2]$[(−)-*O*,*O*′-dibenzoyl-L-tartrate]·$12H_2O$ as the enantiopure building block. The complexation of the oligomeric bibenzimidazoles and the enantiopure building block proceeds with the retention of configuration. To the best of our knowledge, the X-ray structure of the tetra-Ru complex Λ_4-$[(Ru(bpy)_2)_4(bis(BiBzIm))](PF_6)_4$ is the crystal structure of multinuclear Ru assembly with the highest nuclearity reported to date. It reveals that all four Ru centers have Λ configurations and the bridging ligand bis-bibenzimidazole maintains nearly coplanar. The UV−vis and electrochemical properties indicate a weak electronic communication between the ruthenium metal centers.

Experimental Section

Synthesis. All the reactions were carried out in the absence of light as a precaution of photoracemization.

Resolution of $[Ru(bpy)_2(py)_2]^{2+}$.[34,37,40] Disodium (−)-*O*,*O*′-dibenzoyl-L-tartrate Solution (0.5 M). This solution was prepared using a modification of a previously reported procedure:[40] NaOH

(14.0 g) was dissolved in 50 mL of deionized water to make a NaOH solution (C = 7 M). (−)-*O*,*O*′-Dibenzoyl-L-tartaric acid (4.6 g, 12.2 mmol) was dissolved in 20 mL of H_2O to make a suspension. The above NaOH solution (4.3 mL, C = 7 M, 30.1 mmol, 2.47 equiv) was added dropwise to the above (−)-*O*,*O*′-dibenzoyl-L-tartaric acid solution. Stirring was continued at room temperature for 2 h until the pH reached 9.1. (pH around 9.1 is important for the formation of the red crystals described below.)

Λ-[Ru(bpy)$_2$(py)$_2$][(−)-*O*,*O*′-dibenzoyl-L-tartrate] (2). An aqueous solution of disodium (−)-*O*,*O*′-dibenzoyl-L-tartrate (12 mL, 0.5 M, 6 mmol, 3.35 equiv) was added dropwise to a solution of *rac*-[Ru(bpy)$_2$(py)$_2$]Cl$_2$ (1.15 g, 1.79 mmol) in 22 mL of water. The mixture was stirred for 10 min. In a dark room, the solvent was allowed to evaporate naturally. The red crystals formed the next day. After 8−10 days, the red crystals of **2** were collected by filtration, then rinsed with cold water and air-dried. Yield: 0.72 g, 35% (theory: 50%). ^{1}H NMR (500 MHz, DMSO-d_6): δ 9.00 (d, J = 5.4 Hz, 1H), 8.67 (d, J = 8.1 Hz, 1H), 8.59 (d, J = 8.1 Hz, 1H), 8.38 (d, J = 5.4, 2H), 8.22 (dd, J = 8.1, 8.1 Hz, 1H), 8.00 (d, J = 6.7 Hz, 2H), 7.99 (dd, J = 8.1, 8.1 Hz, 1H), 7.92 (d, J = 7.4 Hz, 1H), 7.88 (dd, J = 6.7, 6.7 Hz, 2H), 7.59 (dd, J = 7.4, 7.4 Hz, 1H), 7.47 (dd, J = 7.4, 7.4 Hz, 3H), 7.39 (dd, J = 7.4, 7.4 Hz, 2H), 5.48 (s, 1H). ^{13}C NMR (125 MHz, DMSO-d_6): δ 168.7, 165.4, 157.0, 156.8, 153.3, 152.5, 152.3, 138.0, 137.9, 137.7, 132.3, 131.8, 129.3, 128.2, 128.1, 127.7, 126.2, 124.0, 123.8, 76.9. The tartrate salt was dissolved in methanol and was converted to Λ-[Ru(bpy)$_2$(py)$_2$](PF$_6$)$_2$ by precipitation with the addition of a saturated aqueous solution of NH_4PF_6. Then, Λ-[Ru(bpy)$_2$(py)$_2$](PF$_6$)$_2$ was purified by metathesis with an acetone solution of tetra-*n*-butylammonium chloride to precipitate the chloride salt Λ-[Ru(bpy)$_2$(py)$_2$]Cl$_2$. The CD spectrum is consistent with the published data[37] (CH_3CN, λ, nm, ($\Delta\epsilon$, $M^{-1}\cdot cm^{-1}$)): 250 (−9.5), 278 (−13.1), 294 (+115.5), 364 (−16.3), 445 (−3.9), 502 (+1.4), 524 (+1.2).

Λ-[Ru(bpy)$_2$(BiBzImH$_2$)](PF$_6$)$_2$ (Λ-3). 1[13] (0.11 g, 0.47 mmol) was suspended in 20 mL of ethylene glycol and degassed for 15 min under nitrogen, then heated at 150 °C until it dissolved. Then the solution was cooled to 120 °C, and Λ-[Ru(bpy)$_2$(py)$_2$][(−)-*O*,*O*′-dibenzoyl-L-tartrate] (0.29 g, 0.25 mmol) was added. The mixture was heated at 120 °C for 8 h. The resulting deep red-brown solution was cooled, diluted with 30 mL of water, and filtered to remove the excess bibenzimidazole. A saturated aqueous solution of NH_4PF_6 was added dropwise to the above filtrate to precipitate the crude Ru complexes. The crude was collected by filtration and air-dried (0.17 g, crude yield: 90%). The crude product, which contained **Λ-3a** and **ΛΛ-5**, was deprotonated by $NaOCH_3$/methanol to get the mixture of **Λ-4** and **ΛΛ-5** (see the procedure of **Λ-4**). **Λ-4** was not soluble in acetone and was separated by filtration. **ΛΛ-5** remained in the acetone solution as the PF_6^- salt. Then the pure deprotonated complex **Λ-4** was suspended in methanol and acidified by adding concentrated HCl to get **Λ-3**. Diethyl ether was added dropwise to precipitated out **Λ-3**. It was purified by dissolving in methanol and metathesis with a saturated aqueous solution of NH_4PF_6 to convert to the PF_6^- salt Λ-[Ru(bpy)$_2$(BiBzImH$_2$)](PF$_6$)$_2$. ^{1}H NMR (500 MHz, DMSO-d_6): δ 8.88 (d, J = 8.1 Hz, 1H), 8.78 (d, J = 8.1 Hz, 1H), 8.25 (dd, J = 8.1, 8.1 Hz, 1H), 8.06 (dd, J = 8.1, 8.1 Hz, 1H), 8.01 (d, J = 6.1 Hz, 1H), 7.91 (d, J = 6.1 Hz, 1H), 7.86 (d, J = 8.1, 1H), 7.60 (dd, J = 6.1, 6.1 Hz, 1H), 7.48 (dd, J = 6.1, 6.1 Hz, 1H), 7.38 (dd, J = 8.1, 8.1 Hz, 1H), 7.06 (dd, J = 8.1, 8.1 Hz, 1H), 5.63 (d, J = 8.1 Hz, 1H). CD (CH_3CN, λ, nm, ($\Delta\epsilon$, $M^{-1}\cdot cm^{-1}$)): 238 (−16.8), 254 (40.9), 282 (−124.0), 294 (+185.1), 314 (+64.1), 330 (+85.8), 348 (+78.9), 430 (−26.8), 482 (+7.2).

Λ-[Ru(bpy)$_2$(BiBzIm)] (Λ-4). The crude Ru complexes from the above reaction (0.17 g) were added to 20 mL of methanol, and the suspension was degassed for 15 min under nitrogen. $NaOCH_3$ (0.15 g, 2.77 mmol) was dissolved in 5 mL of methanol and added to the above suspension dropwise. The color of the solution turned from deep red-brown to purple. The solution was refluxed for 3 h under nitrogen. After the resulting mixture was cooled, the solvent was condensed to a half volume by rotary evaporation. Then the mixture, which contained **Λ-4** and **ΛΛ-5**, was filtered and rinsed with acetone to provide the pure solid product **Λ-4**. Sometimes the solid was difficult to collect by filtration due to the small size, and then the following method was applied: the mixture of **Λ-4** and **ΛΛ-5** was suspended in acetone. An acetone solution of tetra-*n*-butylammonium chloride was added dropwise to precipitate the chloride salt ΛΛ-[(Ru(bpy)$_2$)$_2$(BiBzIm)]Cl$_2$ (**ΛΛ-5**) and **Λ-4**, which were collected by filtration. The solid obtained was suspended in water to dissolve **ΛΛ-5**. The deprotonated **Λ-4** was not soluble in water and was separated by filtration. ^{1}H NMR (500 MHz, DMSO-d_6): δ 8.75 (d, J = 8.1 Hz, 1H), 8.64 (d, J = 8.1 Hz, 1H), 8.09 (dd, J = 8.1, 8.1 Hz, 1H), 7.94 (d, J = 6.1 Hz, 1H), 7.86 (dd, J = 8.1, 8.1 Hz, 1H), 7.73 (d, J = 6.1 Hz, 1H), 7.49 (dd, J = 6.1, 6.1 Hz, 1H), 7.41 (d, J = 8.1 Hz, 1H), 7.37 (dd, J = 6.1, 6.1 Hz, 1H), 6.75 (dd, J = 8.1, 8.1 Hz, 1H), 6.45 (dd, J = 8.1, 8.1 Hz, 1H), 5.35 (d, J = 8.1 Hz, 1H). ^{13}C NMR (125 MHz, DMSO-d_6): δ 158.8, 157.6, 157.2, 151.4, 150.8, 148.1, 145.0, 135.2, 134.5, 126.4, 126.3, 123.4, 123.0, 118.6, 118.0, 117.9, 111.1. CD (CH_3CN, λ, nm, ($\Delta\epsilon$, $M^{-1}\cdot cm^{-1}$)): 216 (−74.0), 249 (+31.5), 264 (50.8), 285 (−29.7), 299 (+157.3), 319 (+61.6), 322 (+62.5), 398 (−32.3), 467 (−10.1), 543 (+7.1).

ΛΛ-[(Ru(bpy)$_2$)$_2$(BiBzIm)](PF$_6$)$_2$ (ΛΛ-5). For the above deprotonation reaction, the product which was soluble in water was ΛΛ-[(Ru(bpy)$_2$)$_2$(BiBzIm)]Cl$_2$. It was precipitated by metathesis with a saturated aqueous solution of NH_4PF_6 to convert to the PF_6^- salt **ΛΛ-5**. **ΛΛ-5** can also be prepared in the following one-step reaction: **1** (0.020 g, 0.085 mmol) and **2** (0.21 g, 0.18 mmol) were suspended in 10 mL of ethylene glycol and degassed for 15 min under nitrogen, then heated to 120 °C, and kept at this temperature for 8 h. The resulting deep red-brown solution was cooled, diluted with 15 mL of water, and filtered to remove the insoluble part it may have. A saturated aqueous solution of NH_4PF_6 was added dropwise to the above filtrate to precipitate the crude Ru complex. After being air-dried, the crude was dissolved in acetone, and then diethyl ether was added dropwise to precipitate the desired pure bis-Ru complex **ΛΛ-5** (0.092 g, yield: 80%). ^{1}H NMR (500 MHz, DMSO-d_6): δ 8.79 (d, J = 8.1 Hz, 1H), 8.76 (d, J = 8.1 Hz, 1H), 8.15 (dd, J = 8.1, 8.1 Hz, 1H), 8.06 (d, J = 8.1 Hz, 1H), 8.06 (dd, J = 8.1, 8.1 Hz, 1H), 7.68 (d, J = 6.1 Hz, 1H), 7.52 (dd, J = 6.1, 6.1 Hz, 1H), 7.36 (dd, J = 6.1, 6.1 Hz, 1H), 6.66 (dd, J = 6.1, 3.4 Hz, 1H), 5.54 (dd, J = 6.1, 3.4 Hz, 1H). ^{13}C NMR (125 MHz, DMSO-d_6): δ 159.4, 157.8, 157.6, 152.9, 151.0, 144.9, 136.4, 136.2, 127.2, 126.6, 123.6, 123.5, 121.1, 113.7. MALDI-TOF (*m*/*z*) (PF_6^- salt): 1367 $[M + H_2O]^+$, 1205 $[M - 1PF_6]^+$. CD (CH_3CN, λ, nm, ($\Delta\epsilon$, $M^{-1}\cdot cm^{-1}$)): 213 (−79.4), 249 (−48.0), 299 (+129.9), 314 sh (+84.9), 342 (+72.1), 405 (−45.0), 445 (−30.2), 520 (+26.7).

Λ$_4$-[(Ru(bpy)$_2$)$_4$(bis(BiBzIm))](PF$_6$)$_4$ (Λ$_4$-Ru$_4$-6). Bis(bibenzimidazole) (**7**)[13] (0.050 g, 0.11 mmol) was suspended in 10 mL of ethylene glycol, degassed for 20 min under nitrogen, and then heated at 150 °C for 2 h to dissolve **7**. Then, the above solution was cooled to 100 °C and **2** (0.54 g, 0.47 mmol) was added. The reaction was heated at 120 °C for 8 h. The resulting deep red-brown solution was cooled, diluted with 10 mL of water, and filtered to remove insolubles. Then a saturated aqueous solution of NH_4PF_6 was added

dropwise to precipitate the complex. The crude solid was collected by filtration (320 mg). The crude product (160 mg) was dissolved in a minimum of acetonitrile and chromatographed over a neutral alumina column (21 cm length, 17 mm diameter). The first deep red broad band was collected. The eluate was concentrated to around 25 mL by rotary evaporation, and then diethyl ether was added dropwise to precipitate the desired complex. Yield: 73%. MALDI-TOF (*m/z*): 2551 $[M - 1PF_6]^+$, 2406 $[M - 2PF_6]^+$, 2261 $[M - 3PF_6]^+$, 2116 $[M - 4PF_6]^+$. Anal. Calcd for $C_{108}H_{78}F_{24}N_{24}P_4Ru_4 \cdot 4H_2O$: C, 46.86; H, 3.13; N, 12.14. Found: C, 46.66; H, 2.72; N, 12.17. CD (CH_3CN, λ, nm, ($\Delta\epsilon$, $M^{-1} \cdot cm^{-1}$)): 214 (−95.1), 241 (+40.1), 251 (−32.7), 283 (+83.3), 298 (+60.9), 309 sh (+64.7), 352 (+120.5), 418 (−91.5), 521 (+32.4).

Λ_8-[(Ru(bpy)$_2$)$_8$(tetra-BiBzIm)](PF$_6$)$_8$ (Λ_8-Ru$_8$-8). **9**[13] (0.050 g, 0.054 mmol) was suspended in 25 mL of ethylene glycol, degassed for 20 min under nitrogen, and then heated at 170 °C for 8 h to dissolve the tetra($BiBzImH_2$) ligand. Eventually, it was still partially dissolved due to the rigid structure of the ligand. Then, the suspension was cooled to around 100 °C, **2** (0.516 g, 0.45 mmol) was added, and the mixture was heated at 150 °C for 2 h. $NaOCH_3$ (58 mg, 1.07 mmol) was added to facilitate the full deprotonation. Then, the solution was heated at 150 °C for another 14 h. The deep red-brown solution was cooled, diluted with around 20 mL water, and filtered to remove the insoluble part. A saturated aqueous solution of NH_4PF_6 was added dropwise to the filtrate to precipitate the complex. The solid crude product (300 mg) was collected by filtration. The crude product (150 mg) was dissolved in a minimum of acetonitrile and purified by chromatography with a neutral alumina column (21 cm length, 17 mm diameter) using an acetonitrile solution of NH_4PF_6 as an eluent. The major portion stayed on the top of the column and was eluted slowly by a saturated acetonitrile solution of NH_4PF_6. The eluate was concentrated to around 10 mL by rotary evaporation, and then ether was added dropwise to precipitate the desired complex. Yield: 55%. MALDI-TOF (*m/z*): 5308 $[M - 1PF_6]^+$, 5154 $[M - 2PF_6]^+$, 4999 $[M - 3PF_6]^+$, 4582 $[M - 6PF_6]^+$, 4431 $[M - 7PF_6]^+$, 4278 $[M - 8PF_6]^+$. Anal. Calcd for $C_{216}H_{154}N_{48}P_8F_{48}Ru_8$: C, 48.13; H, 2.88; N, 12.47. Found: C, 43.07; H, 2.68; N, 11.05 (CHN was analyzed under the optimum combustion condition). CD (CH_3CN, λ, nm, ($\Delta\epsilon$, $M^{-1} \cdot cm^{-1}$)): 210 (−23.0), 242 (+35.5), 257 (+17.2), 284 (+70.9), 349 (+32.6), 432 (−34.2), 532 (+10.1).

X-ray Crystallography. Single crystals of Λ_4-Ru$_4$-**6** were grown from the acetone/water solution (2:1) of the complex by slow evaporation under ambient conditions in the absence of light. The sample was composed of very small, weak-scattering crystals. A Leica MZ7 polarizing microscope was used to identify a suitable specimen from a representative sampling of materials. The specimen was then fixed to a nylon loop which in turn was fashioned to a copper mounting pin. The mounted powder was then placed in a cold nitrogen stream (Oxford) maintained at 110 K. A Bruker D8 GADDS general purpose three-circle X-ray diffractometer was employed for sample screening and data collection. The goniometer was controlled using the GADDS software suite (Microsoft Windows 2000 operating system). A full data set was collected; however, the high-angle data were extremely weak and the intensity measurements at high angle are not as reliable as the low-angle data. As a result, R_{int} and R_σ are relatively high. These values reflect the error associated with the high-angle data. To obtain a chemical and structurally correct model, the 2,2′-dipyridyl, PF_6, and acetone molecules were refined with restraints. The Ru and the bridging organic ligand were not restrained. A summary of the data collection, refinement details, bond lengths, and bond angles are provided in the Supporting Information, Tables S1−S3.

Acknowledgment. We thank the Robert A. Welch Foundation for financial support under Grant No. Y-1291. X-ray diffraction was performed at the X-ray diffraction laboratory, Center for Chemical Characterization and Analysis, Department of Chemistry at Texas A&M University. We thank Dr. Joseph H. Reibenspies for solving the X-ray crystal structure of the tetra-Ru complex (Λ_4-Ru-**6**). We also thank Professor Frederick M. MacDonnell and Professor Norma Tacconi at the University of Texas at Arlington for helpful discussions.

Supporting Information Available: COSY and ^{13}C NMR spectra of compound $\Lambda\Lambda$-**5**. X-ray crystallography data, CIF file of the tetra-Ru complex Λ_4-[(Ru(bpy)$_2$)$_4$(bis(BiBzIm))](PF$_6$)$_4$ (Λ_4-Ru$_4$-**6**). This material is available free of charge via the Internet at http://pubs.acs.org.

IC062148A